CIENTIFIC Publishing Limited

Prevention and Treatment of Natural Disasters
https://ojs.ukscip.com/index.php/ptnd

Article

Analyzing the Vulnerability of Residential Buildings in the City of Chaitén: A Focus on an Extreme Event Scenario in a Disrupted River Corridor Following the Cataclysmic Volcanic Eruption of 2008

Carolina Bertin Salazar [1,2], Bruno Mazzorana [1,3,*], Diego Patricio Bahamondes Rosas [1], Gonzalo Duran Vilches [4] and Pablo Iribarren Anacona [3,4]

[1] Laboratorio de Procesos Superficiales, Facultad de Ciencias, Universidad Austral de Chile, Valdivia 5090000, Chile
[2] Escuela de Geografía, Facultad de Ciencias, Universidad Austral de Chile, Valdivia 5090000, Chile
[3] Instituto de Ciencias de la Tierra, Facultad de Ciencias, Universidad Austral de Chile, Valdivia 5090000, Chile
[4] Laboratorio de Geoinformatica, Facultad de Ciencias, Universidad Austral de Chile, Valdivia 5090000, Chile
[*] Correspondence: bruno.mazzorana@uach.cl

Received: 20 February 2024; **Revised**: 15 April 2024; **Accepted**: 17 April 2024; **Published**: 30 April 2024

Abstract: Pillared on the hydrodynamic simulation of an extreme flooding scenario, we subsequently evaluated the physical vulnerability of residential buildings utilizing an ad hoc developed indicator-based methodology. This method aimed to quantify the expected loss for each affected residential structure. The outcome of this assessment facilitated the creation of a detailed risk map, allowing for the identification of hotspots that require immediate prioritization in mitigation efforts. The results of our study revealed a concentrated impact of the flood, particularly in the northern sector of the city. Within this region, four high-risk areas were pinpointed, comprising 70 homes predominantly situated close to the active channel zones. Notably, our findings underscored that twelve residential buildings, located at shorter distances from the river, are particularly susceptible to the impacts of the flood, as indicated by the physical vulnerability index values. It is important to highlight that the developed methodology is specifically tailored for the analysis of lightweight, one or two-storey houses with exteriors constructed from wood and zinc plates, as opposed to structures built with concrete or stone masonry. This distinction is crucial, given the prevalence of such building types in the Chilean Patagonian region. We recommend extending the application of this methodology to other urban areas in the region, where analogous impacts are possible and similar architectural patterns are common.

Keywords: vulnerability; hydrodynamic impact; indicator-based methodology; specific risk

1. Introduction

River floods, increasingly common due to climate change and pervading construction malpractices in flood-prone areas, pose significant risks, causing extensive economic, social, and environmental losses [1]. Recent events, like the Ahr River flood in 2021, highlight the unpredictable nature and widespread impact of these disasters across Central Europe, with specific examples in Germany and Belgium [2,3]. Floods in volcanic areas can have dramatic consequences as they can transport large quantities of organic and inorganic debris thereby increasing the flood damage potential [4] and disrupting fluvial corridors for decades [5]. Multiple strategies have been proposed to assess flood hazards and risks in volcanic areas, although most of them have been implemented at regional or local scales [6,7] but not at the scale of individual buildings. Urbanized areas in Chile

also face a growing flood risk, increasing vulnerability, and potential for substantial damages [8–10]. Notably, the devastating 2015 floods in northern Chile resulted in a state of emergency, causing significant harm to infrastructure and claiming lives. Chaitén, in the Los Lagos Region, experienced a major flood following the 2008 volcanic eruption, modifying profoundly the Blanco River and the city's landscape [11,12]. A recent investigation highlighted ongoing flood risks even without new volcanic activity, emphasizing the need for a flood risk assessment and strategic territorial planning [13]. Risk analysis involves acquiring knowledge to understand threats, vulnerable populations, and affected areas [14–17]. Disaster risk, considering natural or socio-natural threats, is defined by the probability of occurrence and potential impacts [18]. Technical risk analysis involves calculating process probability and damage extent, considering potential damage and vulnerability [18,19]. Vulnerability, the susceptibility of a community or system to threat impact, encompasses physical, social, economic, and environmental dimensions [20,21]. This research emphasizes physical vulnerability, focusing on the starting conditions for physical loss development [22]. With over ninety active volcanoes, it has witnessed significant transformations in numerous river corridors. The distinctiveness of these systems is exemplified by a paradigmatic example, showcasing peculiar process cascades in the recent past. The Blanco River, spanning 70 km^2 with an 18 km length in the Los Lagos Region, faced severe consequences from a volcanic eruption in 2008–2009. The Chaitén Volcano underwent a brief ash emission phase, succeeded by a 15-day Plinian explosive phase and a more extended 20-month effusive event. Refer to [23–27] for detailed eruption information. These volcanic processes significantly altered the riverine environment, affecting land cover, hydrology, and river morphology. Pre-eruption, the Blanco River catchment was primarily covered (84% area) by native forests, including Nothofagus dombeyi, Nothofagus nitida, and Nothofagus betuloides. The river channel averaged 36 m in width with minimal instream large wood [12]. Following the collapse of the volcanic dome in February 2009, an intense flow reshaped the riverine setting. Lahars transported volcanic sediment to the main channel, creating almost vertical and unstable banks of fine volcanic material—ashes and lahars. Reference [24] reported deposition of 4–6 m of ashes across the entire river basin. Vegetation suffered, with hundreds of trees becoming large wood in the river, some remaining standing, and many buried in volcanic sediments [12]. Due to the combined impact of ash deposition and the demise of vegetation, deceased trees lost their inherent ability to naturally stabilize hillslopes and riverbanks. Subsequently, this led to the initiation of multiple slope instabilities and mass movements which contributed significant quantities of both sediment and trees to the river corridor, resulting in the complete aggradation of the river channel [24]. The rise in sea level at the downstream boundary of the alluvial plane further facilitated this aggradation, compelling the flow to reduce its transport capacity [24]. Consequently, extensive flooding occurred in large areas of Chaitén city. During this event, the Blanco River laterally avulsed and incised a new channel, sharply curving to the right and debouching into the sea after a brief straight trajectory. This alteration triggered widespread damages and losses throughout the entire urban area [28]. According to [29], the formation of this new channel devastated approximately eleven blocks and flooded the rest of the city with water, wood, mud, and ash. While there were no human casualties due to the prompt evacuation of the residents, severe damages and material losses occurred, especially in residential buildings. Some of them were completely swept away, while others were impacted by debris of wood and sediments that entered through their openings [29]. In prospect, a crucial point of concern is the "Austral Road" bridge, identified as a critical infrastructure hot spot. Morphological changes along the river, increased sediment and wood supply, and the potential for blockage and loss of conveyance capacity pose a significant flood risk in the urbanized environment.

The residential zones in Chaitén are predominantly defined by modest, single, or two-storey lightweight dwellings. Residential construction commonly employs timber framing, with wood siding serving both aesthetic and functional purposes. Additionally, in contemporary architecture, zinc siding has gained popularity owing to its notable durability, cost-effective maintenance, and enhanced resistance to weathering.

The factors outlined above may give rise to various damage mechanisms that impacted residential buildings could be vulnerable to, including foundation scouring caused by vortex formation at the bases, displacements of affected buildings due to reduced frictional force between the soil and the dwelling, overturning of the dwelling, buoyancy, and collisions with large logs or objects. These mechanisms signify the loss of external stability for the dwellings. Concerning internal stability loss, structural failures of walls due to hydrostatic and hydrodynamic loads from the flow can occur. The ultimate damage mechanism involves the intrusion of water or debris through dwelling openings, potentially causing harm through flooding, contamination, and the deterioration of properties

[30]. While the vulnerability curves, matrices, and indicators developed and reviewed by [31] offer profound insights across a diverse range of scenarios, their applicability to the urban landscape of Chaitén might encounter limitations. This is attributed to the specificity of processes, disparities in construction typologies, and the distinctive damage mechanisms that could potentially be induced in this setting. This study aims to fill this void by presenting a methodology to evaluate physical vulnerability in Southern Chile, specifically focusing on urban zones. The process entails expert elicitation to identify, prioritize, and assign weights to vulnerability indicators. The application of this methodology is demonstrated in the context of Chaitén, specifically considering an extreme flood scenario in the altered river corridor following the 2008 volcanic eruption. All involved experts are familiar with the study area, problem setting and the specific fluvial processes to be considered. Moreover, they participated in the field surveys and contributed to data analysis at various methodological stages. Concretely the addressed research questions were: (a) Which residential buildings in the studied area experience the most pronounced impacts from the flow? (b) How are residential buildings with elevated vulnerabilities distributed spatially? (c) In which high-risk zone is the expected damage more significant? In the following section, we address these queries by first providing a concise overview of the study area and then detailing the specially developed methodology. Following that, we dedicate a section to presenting the results obtained through the application of the devised methodology in the Chaitén case study. Finally, the paper concludes with an in-depth discussion and summarizing conclusions.

2. Materials and Methods

In the preceding section, we highlighted the pivotal role played by the development of an expert-based evaluation method in assessing the physical vulnerability of residential buildings subjected to flooding. In this section, following a concise overview of the study area, we present a hierarchically layered model of all required variables for the quantitative determination of the weights to be assigned to each variable exerting an impact on the physical vulnerability of each impacted residential building. Subsequently, we systematically expound upon all requisite ancillary methodological components, aiming to provide a thorough assessment of each considered variable. Thereupon, we report the employed methodology to quantify the physical vulnerability of the impacted buildings based on the structured hierarchical model with determined weights for each variable, to generate specific spatial vulnerability data. We round off the methodological section by presenting the quantitative assessment of the reinstatement value of the affected residential buildings. Finally, we explain how to generate specific risk maps which visually aid the immediate spatial identification of potential risk hotspots to be eventually prioritized by foresighted risk management activities.

2.1. Study Area

As shown in Figure 1, the research area encompasses the urban area of Chaitén, situated in the Palena province within the Los Lagos region (specifically between 42°55' south latitude and 72°42' west longitude). It includes the Blanco River, originating from the Chaitén volcano, coursing through the city for approximately 18 km before reaching the Pacific Ocean. Encompassing an approximate area of 3 km^2 with an average elevation of 6.4 m above sea level, Chaitén experiences a temperate rainy climate per the modified Köppen classification. This climate lacks a dry season, exhibiting increased precipitation levels during winter, from May to July. The annual average precipitation, recorded by the meteorological station of the General Directorate of Water (DGA - Dirección General de Aguas) operational between 1998 and 2007, is 3408 mm. The study area's flora predominantly features three types of native forests, including evergreen forests with notable species such as Nothofagus dombeyi and Fitzroya cupressoides, as well as high-altitude forests dominated by Nothofagus pumilio and Nothofagus antarctica. In terms of fauna, the region hosts species such as the puma, condor, quique, huillín, chungungo, and coipo [32]. The topography of the Chaitén commune, an extension of the Andes Mountain range, descends sharply towards the sea, characterized by steep hillsides well connected to the Blanco River corridor and fjords [33]. The region features massifs that do not exceed 2500 m above sea level. Notable volcanoes in the area include Corcovado (2300 m above sea level), Michimahuida (2404 m above sea level), and Chaitén (962 m above sea level).

Figure 1. Map of the Study Area comprising the Urban Area of Chaitén, the segment of the Blanco River with its fan delta. Upper left panel: Location of the communal area of Chaitén.

2.2. Setup of a Hierarchically Layered Model to Assess the Physical Vulnerability of Residential Buildings Exposed to Flooding

To assess the physical vulnerability of the residences, the Analytic Hierarchy Process (AHP) method, a multiple criteria approach, was applied. This method allows the analysis and resolution of complex problems integrating the subjective judgment of experts [34]. The technique breaks down complex problems into a hierarchy of elements, effectively identifying their objectives, criteria, and sub-criteria [35]. Once identified, a pairwise comparison is made among criteria and sub-criteria, respectively, thereby assigning a rating ranging from 1 to 10 based on the level of importance or influence one has over the other [35]. In the case of this research, the assigned rating for each criterion was determined through the collaboration of an expert panel consisting of 9 professionals affiliated with the SEDIMPACT project. These experts possess demonstrable experience in natural hazard research and have a profound knowledge of the study area. Figure 2 (see Section 3) illustrates the layered structure of the hierarchical model designed for evaluating vulnerability, representing the core objective variable. The second layer captures the interplay of Process Impacts (quantified by an ad hoc process model) and Buildings Susceptibility, influencing the objective variable directly. The third level encompasses Geometric and Structural Characteristics as well as Building materials, collectively contributing to the Buildings Susceptibility and the Hydrodynamic Impact and the Morphological Changes induced by floods, conjointly contributing to the Process Impacts. The fourth hierarchical level further dissects variables contributing to Buildings Susceptibility. Considered Geometric Characteristics include the Base Area of the building, its Volume, and the featured Number of Openings in the Envelope of the building. Lastly, we examined

the Building Materials used for building exteriors as a proxy for building material quality, distinguishing between Wood, Fibrocement, Zinc Plates, and Masonry Bricks.

2.3. Determining the Importance Weights of the Model Variables

In implementing this method, we employed Klaus Goepel's Excel template for AHP with multiple inputs [35–37]. The template includes a summary sheet presenting the results, 20 input sheets for pairwise comparisons, a sheet for consolidating all judgments, and a sheet with reference tables. The summary sheet provides insights into the weights assigned to each analyzed variable, the absolute errors resulting from comparisons, and the consensus index among experts, expressed on a scale from 0 to 100%.

Building upon the hierarchical structure established for the quantified physical vulnerability objective, experts engaged in pairwise comparisons between variables of the same hierarchical level. Using a scale (typically 1 to 9), they conveyed the relative importance or preference of one variable over another. These comparisons generated square matrices for each hierarchy level, with matrix elements reflecting the assigned relative importance scores. Employed algorithms, such as eigenvector and eigenvalue methods, allowed for the calculation of the weights to be assigned to each variable based on the comparison matrices. The method concludes with consistency checks, ensuring the reliability of expert judgments throughout the comparison process.

Experts were chosen based on their domain expertise, cultivated through at least one year of involvement in a research project funded by ANID (Chilean National Agency for Research and Development) and/or their professional or scientific curricula focused on natural hazards, risk assessment and management and closely related fields. This research project equipped them with a profound understanding of the multifaceted issues integral to the research. These experts actively contributed throughout various stages of the investigation, including the analysis of fluvial processes in the Blanco River, participation in field surveys, and engagement in four project seminars aimed at disseminating updated project knowledge. The diverse training backgrounds of the nine involved experts offered a necessary richness of perspectives. Two of them hold a doctorate in Geography, one holds a doctorate in Forest Engineering. Furthermore, one member of the expert panel obtained a master's degree in Water Management and another one is a doctorate candidate in Forest Engineering. Finally, three members are professional Geographers and one is a professional Geologist. All members of our expert panel informed both, the physical vulnerability of residential buildings and the hydrogeomorphic process impact, based upon their professional experience and their knowledge of the hydrogeomorphic processes affecting the Blanco River after the 2008 eruption. To ensure a comprehensive understanding of the AHP methodology, a joint seminar dedicated to its application was held, complemented by video tutorials for troubleshooting.

2.4. Quantifying the AHP Model Variables

Employing a Mavic 2 Pro drone and EMLID REACH RS+ GPS, we conducted a photogrammetric survey in Chaitén, creating a Digital Elevation Model (DEM) for simulating an extreme flood scenario. Focusing on the Blanco River and Chaitén's urban zone (see Figure 1), we subdivided the area into 15-hectare parcels for a 5cm/pixel resolution. Each parcel underwent three drone flights with different camera angles to enhance 3D reconstruction. Ground control points (GCP) were used, with 5 points in each parcel polygon. Cross-sectional profiles in the river channel were surveyed for a precise bathymetric representation of the flow areas. Agisoft Metashape processed 7000 images on a computer with an Intel Core i5-9600K processor and 48 GB of RAM generating a dense point cloud. To conduct the hydrodynamic simulations, a DEM and orthomosaic were created, providing a digital terrain model with a 0.2 m pixel size and a 1.28 km^2 calculation grid extension (i.e., computational domain).

To further optimize hydraulic simulation models, we reduced the study area and increased the pixel size. The DEM had irregularities in areas of buildings, so we drew the geometries of the buildings and added an arbitrary elevation to ensure a more realistic representation of the surface. This did not affect the simulations as the flow depth did not exceed 2 m in the city [38]. Granulometric data were obtained through the photogrammetric technique. Based on 11 riverbed photos (i.e., quadratic frames of 1 m^2 riverbed surface) and subsequently employing the Structure from Motion technique conducive to a granulometric analysis, a mean diameter of 40.5 mm could be estimated. To obtain this value, the elements composing the bed material were

identified and their diameter was measured from the riverbed photos using the software tools Digital Gravelometer [39], Split and Basegrain [40] allowing for a granulometric curve representation of the bed material. The roughness coefficient (CR) is crucial for hydrodynamic simulations. It was defined using tables proposed by [36], widely adopted by researchers and practitioners in the field. For floodplain areas, a hybrid methodology combining previous approaches and Chow's method was applied [41]. Roughness values were assigned to land-use types as follows: 0.048 to active channel areas, 0.08 to levees revested with cyclopic boulders, 0.014 to road pavements, 0.2 to residential areas with buildings, 0.25 to forested areas, 0.02 to fine tephra deposits, 0.025 to grassland, 0.02 to barren soil.

Structures interacting with the flow including bridges and houses were individually surveyed and integrated into the calculation mesh. Two main sets were identified: the Austral Road bridge (deck and pillars) crossing the Blanco River and 715 residential buildings, respectively.

The geometry of the Austral Road bridge accurately reflects the dimensions outlined in the original project plans. Conversely, for the potentially exposed residential buildings, their geometric attributes were established by adjusting a circumscribing polygon to their base area. Initially, the houses were delineated manually using the ortho-mosaic obtained from 3D modeling interpreting the images at a scale of 1:180. Geometrically, the Base Area of the houses is represented by four-sided polygons. Additionally, onsite measurements were conducted to calculate the building Volume and annotate the Number of Openings in the Envelope.

Regarding Geometric Characteristics, experts emphasize that the wetted area of each façade of the impacted buildings crucially influences the magnitude of the Hydrodynamic Impact. They argue that the Number of Openings, such as doors and windows, constitute structural weak points, as they permit easy entry for both liquid and solid fluxes. The Vulnerability of residential buildings to potential damage is intricately tied to their Structural Characteristics as well. In addition to the aforementioned Geometric Characteristics—Base Area, Volume, and Number of Openings—experts underscored the critical importance of the Type of Foundation. This factor is pivotal in determining the external stability of the building. Experts discerned in this respect between raft foundations (i.e., Radier Foundation), Concrete Pillars and Wood Pillars. Finally, experts attributed a special role in determining the building's vulnerability to the employed Building Materials, particularly those of the outer layer of the building envelope, namely Wood (i.e., timber) or Fibrocement elements, Zinc Plates or Masonry Bricks (i.e., bound together with mortar). Of particular concern is the prevalent use of simple timber framing in rural areas like the study site of Chaitén. These frames, often lacking a specific design for resistance to horizontal impact forces, are commonly employed in constructing walls of residential buildings. Consequently, when the outer layer materials fail, the timber framing is unable to provide further resistance against flooding. The characterization of both the Type of Foundation and the Building Materials utilized was carried out through careful visual inspection.

Given the scarcity of hydrological data and the disparities in results across previous studies, in this work, we decided to take as a reference upstream boundary condition a worst-case flooding scenario. This scenario was designed to: (a) significantly surpass the discharge values reported by the aforementioned studies and (b) unfold within the context of volcanic perturbation affecting the river corridor. By considering only one reference impact scenario a comprehensive risk quantification is impossible. Such an assessment would require the construction of an expected damage function based on several impact scenarios (with known return period). Instead, we quantify an extremely specific risk scenario contingent upon the occurrence of a specified worst-case flooding scenario. Such a specific risk scenario should be viewed as a valuable counterfactual, aimed at challenging preconceived notions about risk and prompting a critical examination of proposed risk management strategies, potentially leading to their enhancement.

Accordingly, we established an incoming discharge of 700 m^3/s for the Blanco River and 50 m^3/s for the Chai-Chai River (tributary) with a duration of 10,000 s. We used a discharge of 300 m^3/s for simulations as this is the value required to overtop the levees of the Blanco River. This discharge in the order of magnitudes of catastrophic lahars albeit likely overestimating the maximum discharge of the event occurred in the Blanco River. This choice is justified since our hydrodynamic simulations were not able to capture appropriately the extent of the backstepping aggradation which took place and triggered the channel outburst at a lower discharge level. Therefore, we also envisioned a 1-meter elevation increase across the entire riverbed. This adjustment simulates a massive accumulation of volcanic material, thereby establishing initial conditions somewhat akin to those of the event of 2008. Simulations were conducted with the freeware software Iber which is a hydrodynamic

simulation model that utilizes the Saint Venant 2D equations [42] providing for a full representation of flow depths, velocities, and bed elevation changes within the defined computational domain thereby allowing for a complete representation of Process Impacts according to considered variables in the AHP model represented in Figure 2. For a detailed description of the model implementation in the study area the reader is referred to [43]. Endowed with the quantified flow variables for the assumed worst-case flooding scenario, we quantified the Hydrodynamic Impact on the facades of the impacted residential buildings. To this aim, the Specific Normal Force equation proposed by [1], based on an extensive experimental program and precise measurements of impact forces on a vertical plate, was applied in Equation (1):

$$f = 4.47492 \cdot h + 2.29447 \cdot h^2 \quad (1)$$

Here, f represents the specific normal force (in kN m^{-1}) normal to the façade and h in m is the flow height of the approaching flow. It is crucial to note that the results obtained were converted to N/m^2. After conversion, the maximum impact values for each building envelope were selected.

2.5. Assessing the Physical Vulnerability of the Exposed Buildings and Generating a Specific Risk Map

The physical vulnerability of an exposed building is evaluated as a linear weighted sum expressed in Equation (2) as follows:

$$V_i = \sum_j^n w_j \cdot v_{ij} \quad (2)$$

wherein V_i is the quantified vulnerability value of the ith building, w_j is the importance weight assigned to the jth variable through the employed expert elicitation method according to the adopted hierarchical structure of the AHP model and v_{ij} is the value of the jth variable expressing a specific impact for or a susceptibility of the ith building.

To apply this method the values of non-categoric variables (i.e., Base Area, Volume, total Number of Openings, Hydrodynamic Impact, and Morphological Change) need to be normalized by dividing each calculated value of the variable by the respective maximum in the available dataset.

The Expected Damage for a specified residential building contingent upon the occurrence of the reference extreme flooding scenario is calculated by multiplying its Vulnerability by its Reinstatement Value. The determination of the Reinstatement Value entails a thorough technical and economic analysis of the construction processes necessary to reconstruct a building to its original state, or the closest approximation achievable. Each type of intervention represents an expenditure category, potentially subdivided into subcategories. The specific interventions encompassed within each category or subcategory are referred to as works or tasks. The total cost is calculated by summing the quantities of each task multiplied by their corresponding prices. Concerning the Chilean construction context [39] provided an ad hoc and up-to-date price and workflow analysis.

3. Results

3.1. Determining the Weights of the AHP Model for Vulnerability Assessment

Hereafter we report the results of the expert assessment of the weights associated with each variable considered in the AHP Model structure (see Figure 2). To reiterate, variables featuring higher weights carry greater importance in determining the physical vulnerability of exposed buildings, while those with lower values have a lesser influence. According to the experts, Process Impacts (0.725) have a greater impact on vulnerability compared to Buildings Susceptibility (0.275). For Process Impacts, the highest weight was assigned to the Hydrodynamic Impact (0.655). The weight of Morphological Change was evaluated, by comparison, with a much lower value (0.345). The Buildings Susceptibility was determined by the weights of its constituting variables, that is Geometric Characteristics with a weight of 0.119, Building Materials with a weight of 0.369, and Structural Characteristics with a weight of 0.512, with the latter holding the highest importance. The weights of the variables contributing to the influence of the Geometric Characteristics were quantified as follows: Base Area (0.328), Volume (0.271), and Total Number of Openings (0.401). Weight assignments for the variable Structural

Characteristics (i.e., Type of Foundation) resulted in: Concrete Pillars (0.382), Radier Foundation (0.202), and Wooden Pillars (0.416). Finally, the importance of Building Materials (i.e., Type of Building Material) was determined by the weights of the associated explanatory variables, that is: Wood (0.196), Fibrocement (0.300), Zinc Plates (0.377), and Masonry Bricks (0.127).

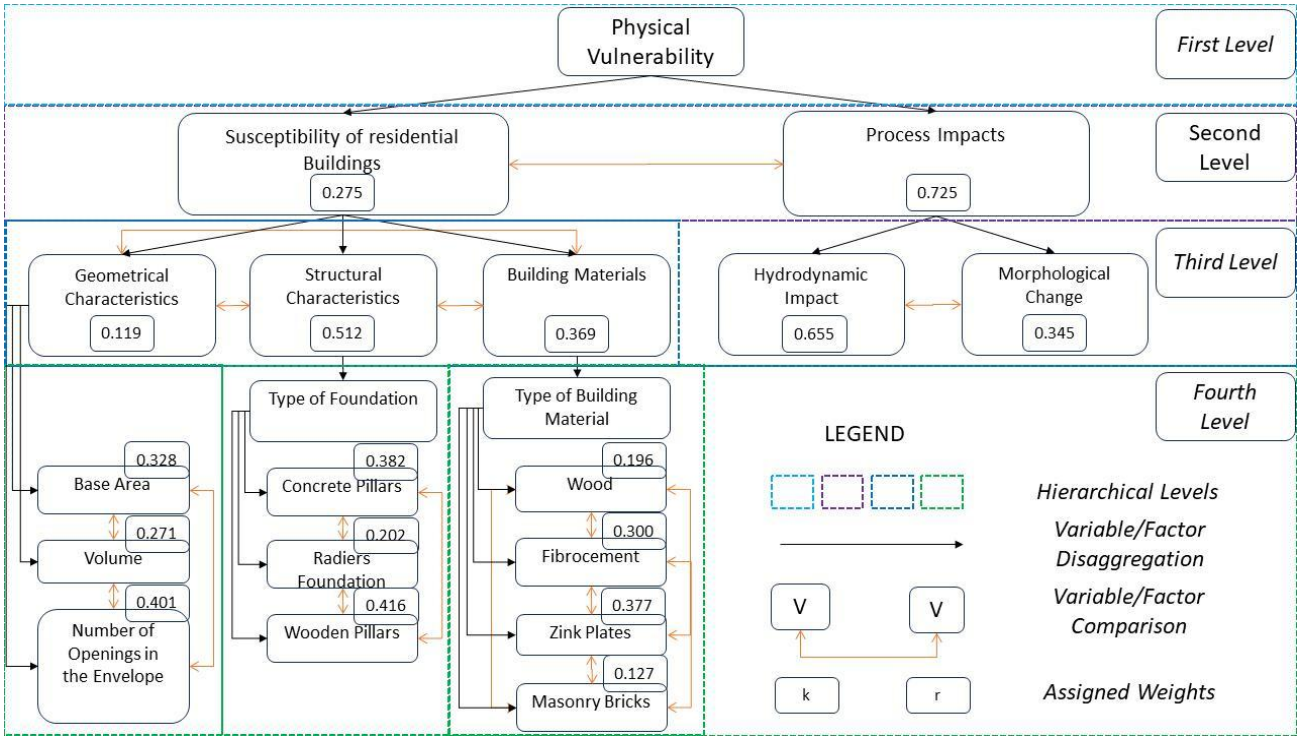

Figure 2. Hierarchical model for physical vulnerability assessment presenting the layered structure of the considered variables (i.e., associated with each of the four hierarchical levels), the top-down disaggregation into explanatory variables/factors (i.e., arrows) and the different variable importance comparisons within each level (i.e., bidirectional arrows). Weights associated with the variables constituting the AHP model used to quantify the vulnerability of exposed residential buildings are also shown.

3.2. Assessing the Process Impacts

The hydrodynamic simulations for a specific flow scenario of 750 m^3/s reveal that 253 buildings are affected by flow depths exceeding 0.1 m. The flooding primarily encompasses the Northern Sector of Chaitén. This area is particularly vulnerable due to its proximity to narrower river sections (refer to Figure 3). Here, the flow is capable to overtop the levee, which was constructed in recent years to safeguard urban areas from the impacts of severe flooding (Figure 3A). Sewer culvert outlets integrated into the crest of the levee can exacerbate this phenomenon (see Figure 3B) augmenting the flow diverted directly towards the inhabited areas. The simulation results illustrate how the inundation progresses along the gridded urban road network within the Northern Sector of the town before ultimately draining into the sea to the south. Geomorphologically, the downstream river reach comprises a dynamic fan-delta, where flow patterns can swiftly and unpredictably change (Figure 3C).

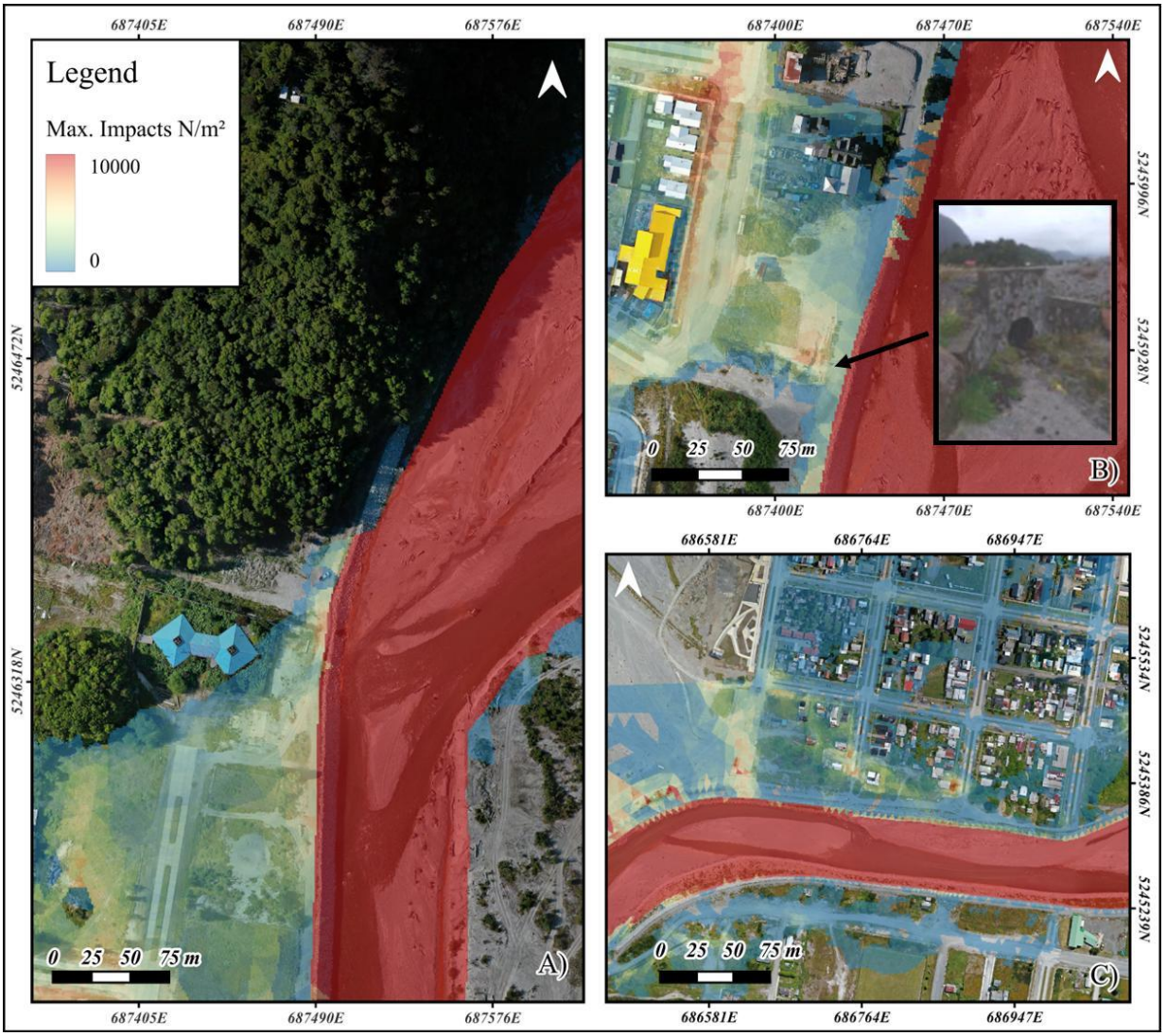

Figure 3. Flood overflow zones in urban areas. (**A**) Channel narrowing; (**B**) Sewer system; (**C**) Flow patterns through the urban areas and at the river mouth.

As illustrated in the flow depth map (refer to Figure 4A), urban areas most vulnerable to substantial flow depths lie adjacent to the Blanco River in the northeast. Here, maximum flow depth values range between approximately 0.7 to 0.9 m. Furthermore, zones with elevated flow depths are located towards the northwest zone of the city and adjacent to the most distal sections close to the river mouth, where depths peak at 0.8 m. Elsewhere in the city, depths vary between 0.1 to 0.5 m, with negligible values along the coastline. Despite the relatively modest flow heights in these urban zones, they still present risks such as water infiltrating buildings. In Figure 4B, the map showcases the peak flow velocities, which can reach 2.8 m/s, particularly along the river and preferred overland flow paths linked to overtopping locations. These flow areas of intense velocity can pose a significant threat, capable of causing severe structural damage and immediate danger to residents.

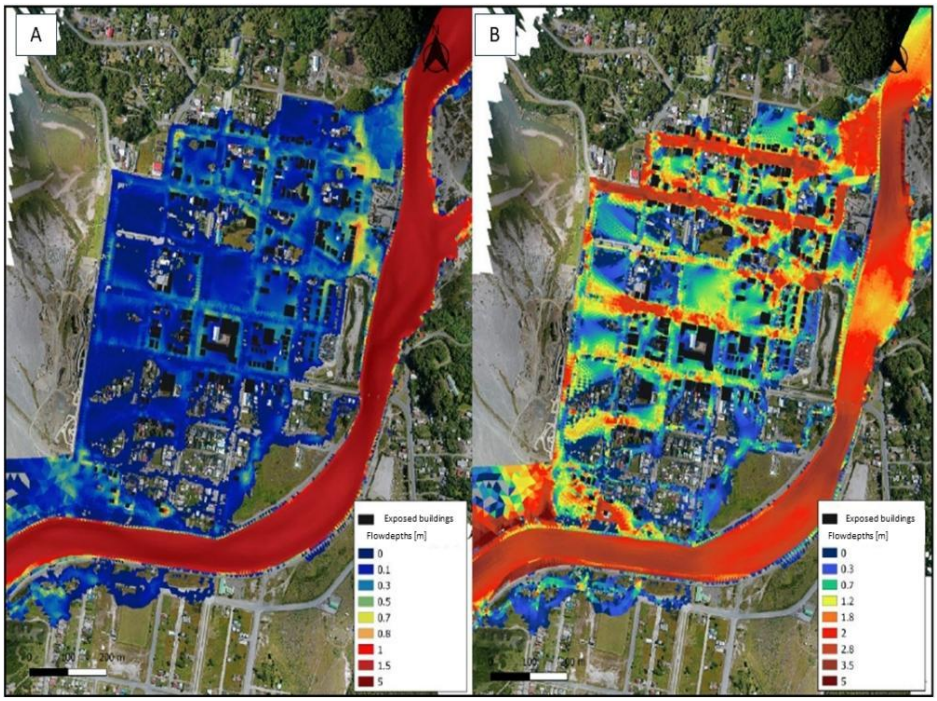

Figure 4. Innundation maps. (**A**) Flow depth cartography (m); (**B**) Flow velocity cartography (m/s).

The propagation of the flow through the built environment allows for the identification of at least four zones of great danger (see Figure 5) to be prioritized for the subsequent vulnerability and specific risk analyses: zones 0, 1, 2, and 3. These areas encompass a total of 90 buildings, of which 70 are residential and 20 correspond to non-residential uses, including institutional buildings. Zone 0 is located northeast of the northern sector of Chaitén and features a total of 50 homes. The second zone is situated in proximity to the river, comprising 3 residences. Zone number 2 is in the northwest and includes 6 residential buildings. Lastly, zone 3 is located near the delta with 10 homes.

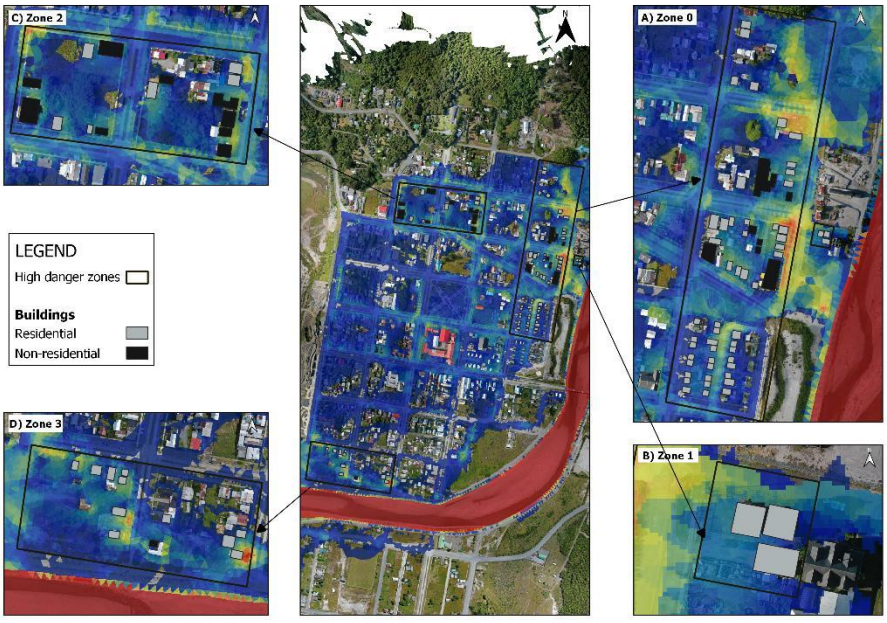

Figure 5. Central Image: Location Four Priority Zones, 0, 1, 2, and 3 respectively. A–D represent enlarged views of the Four Priority Zones. Residential and Non-residential Buildings are dashed in grey and black, respectively.

In Figure 6A, a histogram shows the counts of the residential buildings falling into each interval of the Hydrodynamic Impact. As a proxy we use the Specific Normal Force. Notably, the results demonstrate a positively skewed distribution, indicating that higher values are more widely dispersed compared to their lower counterparts within the range of variability of the calculated Specific Normal Force values. This range of Specific Normal Force values spans from a minimum of 65.7 N/m^2 to a maximum of 802.8 N/m^2, with a median value of 284.4 N/m^2. Furthermore, the histogram highlights that the most frequent occurrences are concentrated between 150 and 300 N/m^2, with a declining frequency observed as the Specific Normal Force values increase, particularly notable within the range of 550 to 620 N/m^2. Additionally, it is imperative to acknowledge the presence of outliers that deviate from the general data trend, as evidenced by an increase in counts for the highest Specific Normal Force intervals.

In Figure 6B, the spatial distribution of Specific Normal Forces overlays the impacted sector of Chaitén. Regions exposed to higher Specific Normal Forces are highlighted in red, while those with lower impact are shaded in blue. Buildings primarily affected by the flow are concentrated in zone 0, where the Specific Normal Force values approximate 625 N/m^2. Zones 1 and 3 demonstrate medium impact levels, hovering around 375 N/m^2, whereas the lowest Specific Normal Force values, ranging from 250 to 125 N/m^2, are observed predominantly in zone 3.

In Figure 7C, the histogram shows the counts of the residential buildings falling into each Morphological Change magnitude interval. Positive values indicate erosion, while negative values indicate sedimentation. Overall, according to the data, households do not experience significant morphological change. 42 buildings show null values or values below 0.05 m of sedimentation or erosion. The process that most affected the households corresponds to erosion, with 4 households experiencing terrain level variations through erosion between 0.10 and 0.24 m. Moreover, 8 households exhibited erosion between 0.05 and 0.08 m. Conversely, 2 households were affected by an appreciable sedimentation thickness (i.e., depositions between 0.07 to 0.11 m), and 3 by low sedimentation (i.e., depositions between 0.05 to 0.08 m).

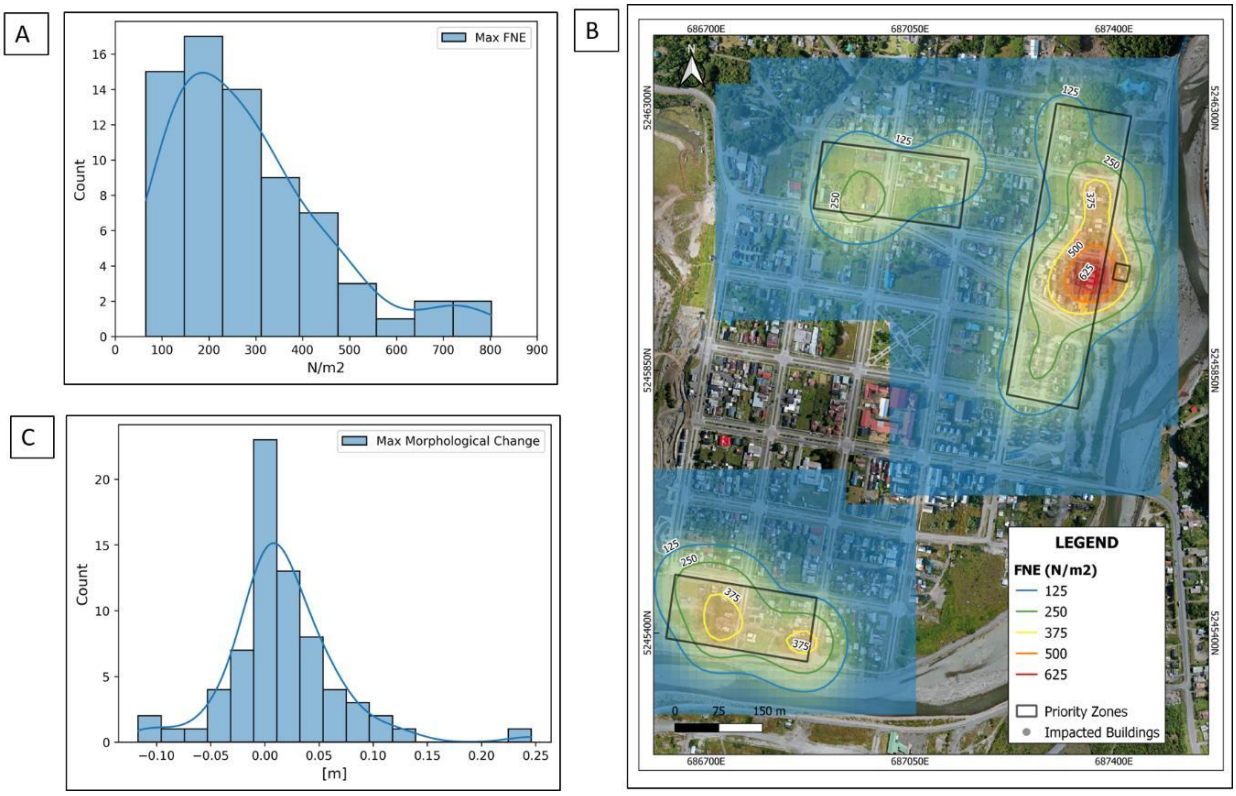

Figure 6. Determination of the flood impact. (**A**) A histogram showing the counts of the residential buildings falling into each interval of Specific Normal Force; (**B**) Spatial distribution of Specific Normal Forces which overlay the impacted sector of Chaitén; (**C**) Histogram depicting the counts of the residential buildings falling into each morphological change magnitude interval.

3.3. Exploring the Susceptibility Variables

In Figure 7A–C, respectively, we depict the histograms showing the counts of the residential buildings falling into specified intervals of Base Area, Volume, and Number of Openings in the Building Envelope.

Base Areas range from 47.9 to 199.18 m^2, with a peak count observed between 47.9 and 78.52 m^2. The counts decrease progressively in the remaining intervals, particularly beyond 160 m^2. Thus, it is evident that a significant number of affected households in the study area have small Base Areas. Regarding the Volume of the buildings under consideration (see Figure 8B), it ranges from 13 to 699.3 m^3, with high counts observed between 110 and 268 m^3. Noticeably, also relatively large building volumes up to 700 m^3 are observed. With respect total number of openings (see Figure 8C), the majority of households have between 10 to 14 openings (60%), while 32.9% fall within the range of 15 to 22 openings.

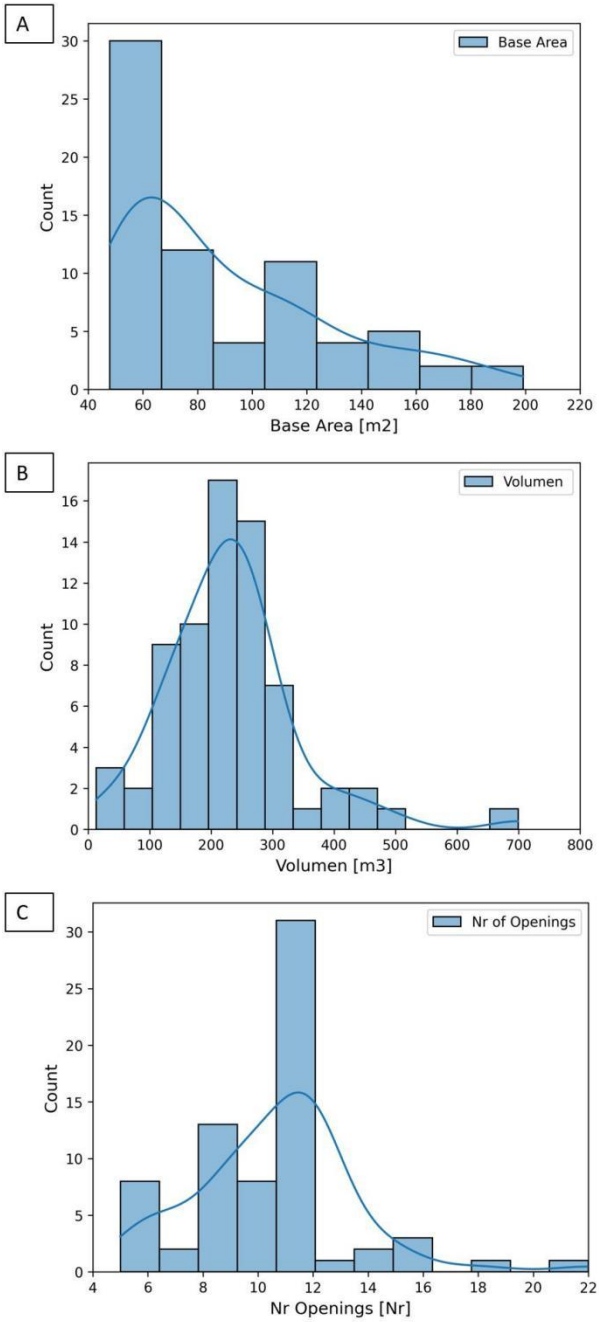

Figure 7. Histograms with the counts of the residential buildings falling into specified intervals. (**A**) Base Area; (**B**) Volume; (**C**) Number of Openings in the building envelope. The blue line indicates a fitting distribution curve.

Concerning the categorical variables exerting an influence on the building's susceptibility the surveyed data evidence the following (see pie charts in Figure 8A,B, respectively). The predominant types of foundations are Radier Foundation (70%), followed by Concrete Pillars (21.4%), and Wooden Pillars (8.6%). According to experts, the latter two foundation types are more susceptible to experiencing some form of damage, thus increasing the vulnerability of the households (see Figure 8A).

As for the Building Materials, envelopes are primarily constructed with Wood (64.3%), followed by Fibrocement (24.3%), and lastly, Zinc Plates (11.4%) (see Figure 8B). It has to be noticed, that Wood has remained a fundamental choice as a building material in the architectural context of the city since the arrival of "Chilote migrants" to the area.

The conservation Status of the building envelopes was considered in more detail (see Figure 8C). The results indicate that the condition ranges from impeccable (i.e., Excellent Condition) to Deteriorated. A 78.6% of residential buildings' envelopes exhibit an Excellent Condition, 20% show a Moderate Condition, meaning they are structurally well-preserved but lacking maintenance, and 1.4% of the households are Deteriorated, with cracks and poor condition of their materials.

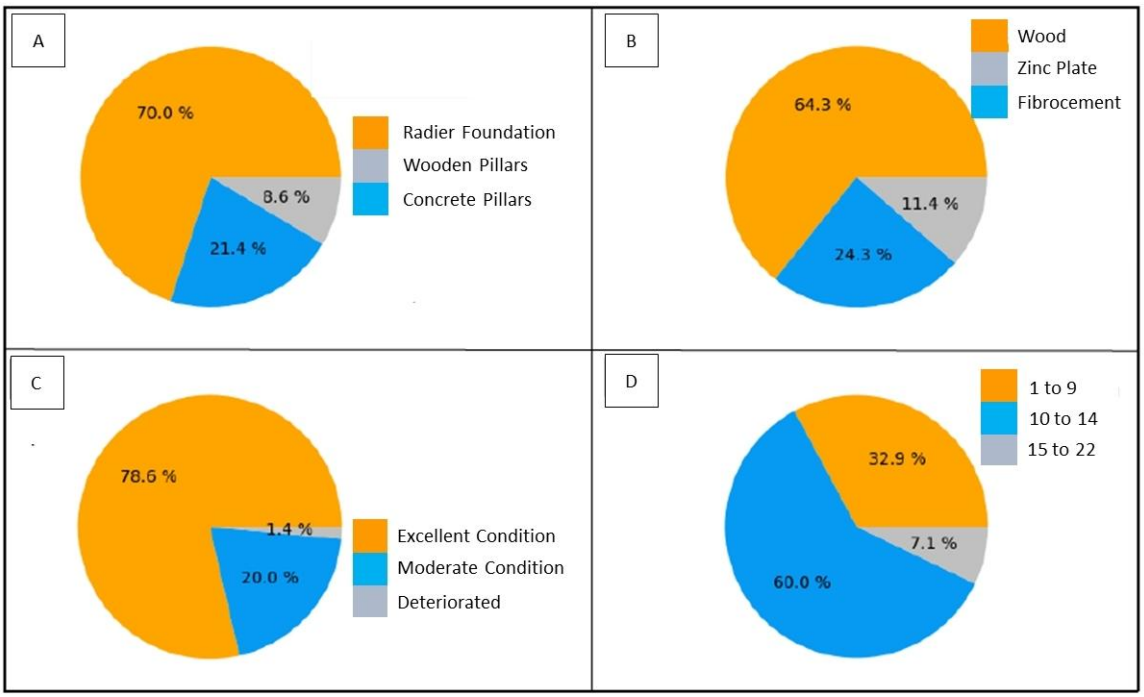

Figure 8. Characterization of the residential buildings. (**A**) Pie charts of the predominant types of foundations; (**B**) Building materials constituting the envelope; (**C**) Their condition; (**D**) The Number of Openings.

3.4. Assessing Normalized and Weighted Process Impacts, Buildings Susceptibilities and Vulnerabilities

Having determined for each considered building both the Susceptibility variables and the Process Impact variables according to the structure of the AHP model in this subsection we present in the form of histograms the normalized and weighted values of both the aggregated Process Impacts (i.e., conjoint influence of both the Specific Normal Force and the Morphological Change), the influence of the aggregated Buildings Susceptibility (i.e., determined by the Base Area, Volume, Number of Openings as well as the elicited Structural Characteristics and surveyed Building Materials) and the resulting Vulnerabilities (see Figure 9A – C, respectively). For the normalized and weighted Process Impacts values between 0.1 and 0.3 clearly predominate, it is noticeable the values of the Building's Susceptibility spike in the interval 0.22–0.24 and are much lower in the other intervals. Hence, expectedly, the building counts are higher for the lower Vulnerability value intervals and decrease progressively for higher Vulnerability value intervals.

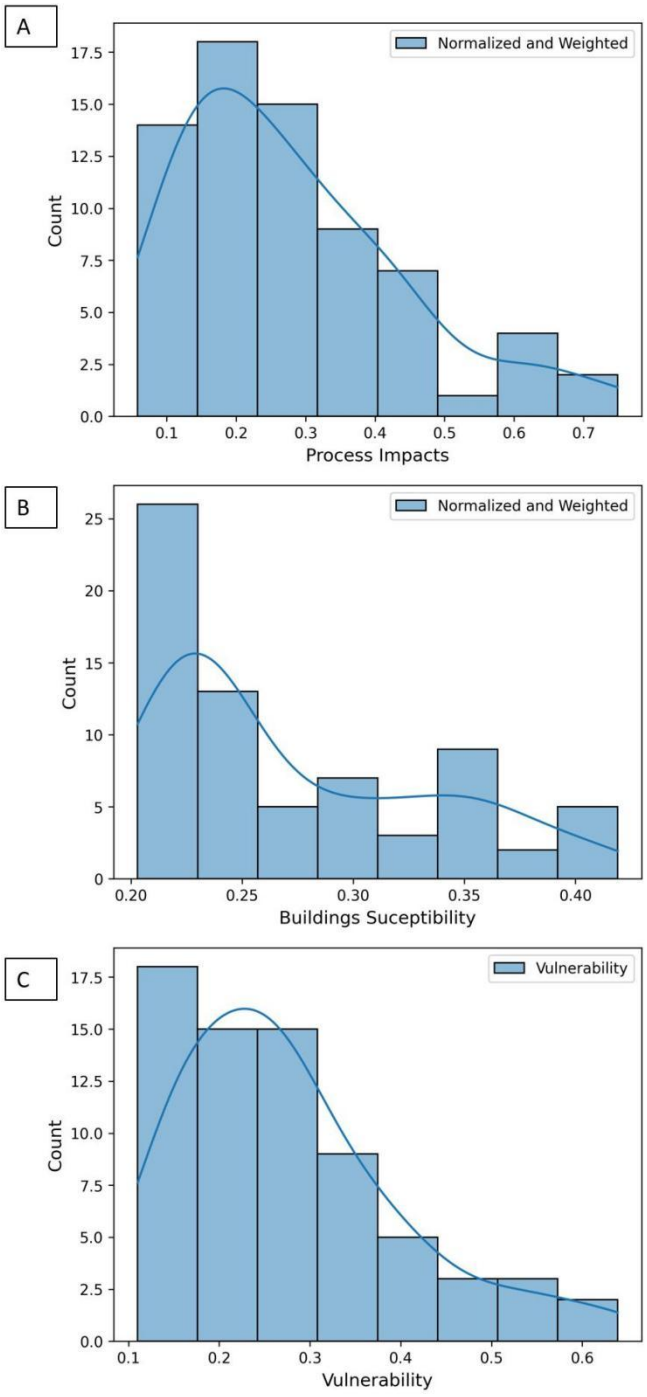

Figure 9. Histograms with the counts of the residential buildings falling into specified intervals of the Normalized and Weighted Process Impact. (**A**) The normalized and weighted buildings susceptibility; (**B**) The resulting Vulnerability; (**C**) The blue line indicates a fitting distribution curve.

In Figure 10A, we present a Bivariate Kernel Density Plot for the Process Impacts versus the Buildings Susceptibility. The contour lines clearly indicate that particularly high building densities fall into the region with Process Impacts less than 0.4 and Buildings Susceptibility comprised between 0.20 and 0.26. Other, albeit remarkably smaller, density peaks, can be found and different Process Impact levels in the Buildings Susceptibility interval 0.33–0.42. Due to the different contributions of Process Impact and Buildings Susceptibility according to the variable weights obtained through the AHP Process it can be noticed (see Plot in Figure 10B) that low to intermediate vulnerability values (i.e., less than 0.44) are associated to the highest kernel

density region. It should not be disregarded, however, that the vulnerabilities associated with the minor kernel density regions can be high (i.e., larger than 0.55) if the Process Intensity is larger than 0.65. In general, very high vulnerability values (i.e., larger than 0.55) can be expected whenever the Process Impact is larger than 0.64 and the Buildings Susceptibility is larger than 0.25 underscoring again the different expert judgement in relation to the importance of the two variables.

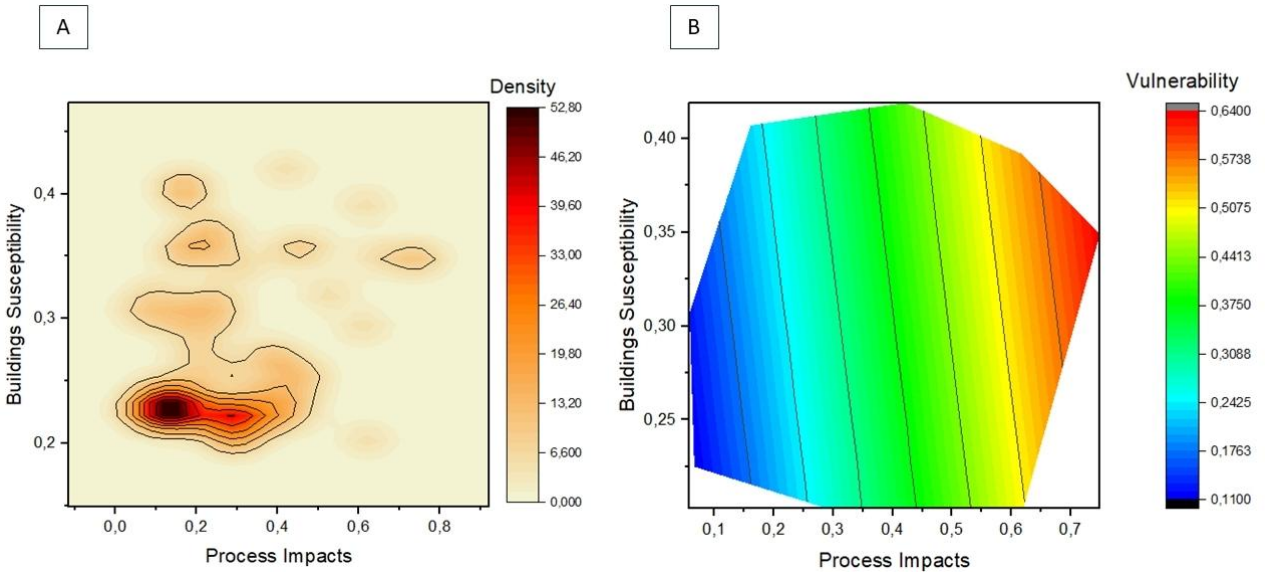

Figure 10. Buildings Susceptibility vs. Process Impact. (**A**) Bivariate (i.e., Process Impacts versus Buildings Susceptibility) Kernel Density Plot; (**B**) Plot showing the Vulnerability values associated with both Process Impact and Buildings Susceptibility values, respectively.

Mapping the Specific Risk for a particular flood scenario requires determining the Expected Damage (i.e., economic value) for each residential building and visualizing it spatially. The Expected Damage values are given by the product of physical vulnerability and reinstatement value. As indicated, Figure 11A, displays the Vulnerability values per building in the four priority zones and in B of Figure 11 the Expected Damage values per building are visualized. Buildings colored in red feature Expected Damage that is very high, ranging from CPL 9.232.139 to CPL 23.180.594. Most of the buildings within this range of Expected Damage exhibit higher Reconstruction Values. Regarding vulnerability levels, these range from low to very high. Buildings with high (CPL 5.994.850–CPL 9.232.139) and medium (CPL 3.583.207–CPL 5.994.850) Expected Damages Values are visualized in orange and yellow, respectively. The associated Vulnerability are similar to the previous group; however, Reinstatement Values are lower. For the lowest Expected Damage level (i.e., CPL 1.730.247–CPL 3.583.207), both Reinstatement Values and Vulnerability levels are low to medium. Analogously to the physical Vulnerability, the Expected Damage does not exhibit a homogeneous spatial pattern; nevertheless, it is possible to observe that 11 of the dwellings with a very high level of Expected Damage are located in particularly high-flow impact areas.

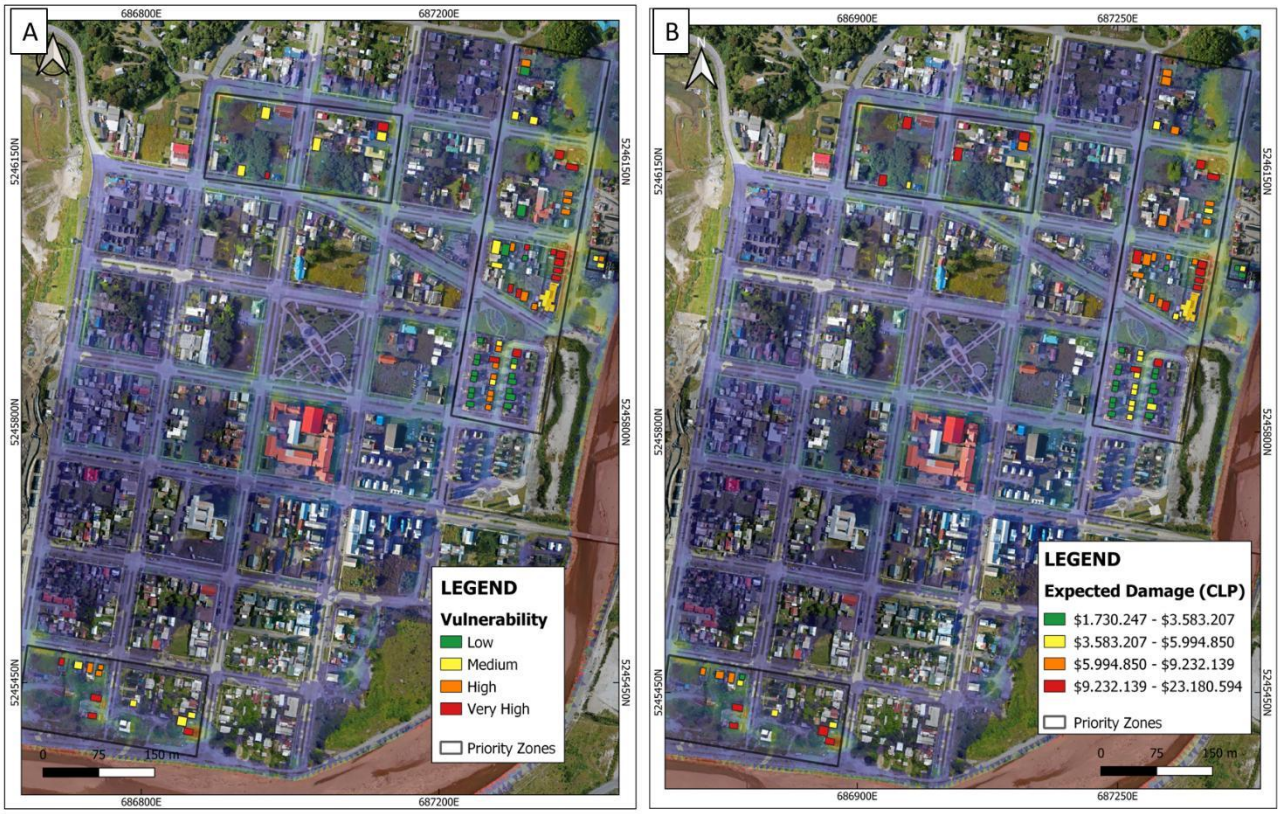

Figure 11. Vulnerability and Expected Damage maps. (**A**) Vulnerability Values per building; (**B**) Expected Damage values per building (damage in Chilean Pesos).

4. Discussion

Chaitén, situated within the Los Lagos region, faced severe repercussions from a significant flood event, resulting in substantial economic setbacks. This calamity garnered attention from a diverse array of researchers aiming to comprehend the dynamics of eruption, hydrological processes, and their impacts on infrastructure. While none of the investigations offers a holistic evaluation of built environment vulnerability and associated risks, one study addressing this at least partially is the work conducted by [29]. This study computed discharge rates for floods occurring at return intervals of 30 and 100 years. Furthermore, it simulated flood extents, factoring in potential obstruction effects on the Austral Road bridge. Moreover, the study quantified performance metrics such as Specific Normal Force and Buoyancy Force for 13 residential structures. Aware of the limitations of their study, [29] argued that a tailored methodology for vulnerability and risk assessment suitable for the regional architecture was still missing. This statement constituted a starting point for this research endeavor. Ideally, as [44] pointed out, such a methodology should allow for a thorough process-structure interaction analysis as performed by [22] for one building only. This analysis presupposed an in-depth knowledge of the building's condition (i.e., precise geometry, complete assessment of the building materials and their condition etc.) and the use of a suite of computational tools such as a hydrodynamic simulation and a finite element structural analysis model. For a large set of buildings such an approach is unfeasible. Recently statistical models allowing for an enhanced vulnerability assessment of residential buildings have been proposed and applied in different contexts [32,45]. As argued in the introduction section, the specificities of the regional architectural context and the peculiar characteristics of the impacting processes constitute an obstacle to using the latter methods in this study. Therefore, we generated a tailored and case study specific vulnerability assessment model by employing the AHP method. Our model relies on expert knowledge both for the definition of its structure (i.e., linkages between variables) and the importance of weighting for each considered variable. Working with expert judgements brings about problems but also valuable insights. Problems were obviously during the initial stages of the AHP, the potential disagreement among experts about the potential damage mechanisms that could affect

the built environment, the different appreciation of the importance of the considered variables. This initial misalignment, however, fueled a focused knowledge integration process. Discussing the AHP model structure, experts underpinned their choices by referring constantly to the specific mechanisms provoking the loss of external and internal stability of the considered structure and its constituting elements. Of course, the persistence of biases cannot be completely excluded, and a different group of experts might have produced slightly different judgements. A potential methodological enhancement could be brought about by letting two groups of experts independently go through the AHP steps. The documentation of the two independent AHP exercises could highlight critical procedural moments where biases might affect the outcomes profoundly.

Experts identified also damage generating mechanisms not linked to any stability loss like those related to fluxes entering through openings in the building envelope. Hence the structure of the setup AHP model is somewhat reminiscent, albeit not explicitly, of the mechanisms at play. It has to be pointed out, however, that the need for a fully physically based process-structure interaction persists particularly for mitigation design aiming at interfering favorably with the damage generating mechanisms.

The considered extreme scenario revealed that the area most affected by the flood corresponds mainly to the northern sector of the urban area of the city, where the overflow begins and extends until reaching the delta. As a result, four residential zones at high risk were identified, mainly located near the Blanco River (zones 0, 1, and 3), except for zone 2 located in the northwest of the city. Although flood heights in the urban area do not exceed 1 meter, they are considered sufficiently high to cause damage to exposed buildings. The behavior of the modeled flow resembles the scenario of a 100-year event with a 50% obstruction of the bridge, simulated by [29], where the northern sector of the city is mostly flooded.

The results derived from the analysis of Specific Normal Force Impact reveal a clear correlation between flow heights near residences and impact forces, as reported by [1]. Maximum Hydrodynamic Impact values (i.e., Specific Normal Forces) were observed in residential buildings adjacent to the river, exceeding 500 N/m^2.

One source of uncertainty in impact assessment is the simplification of geometries (i.e., planform) to four-sided polygons, which may not adequately capture flow behavior during flooding, as noted by [24]. Additionally, it is important to note that the response of surrounding buildings can alter flow patterns, potentially altering impact forces, as documented by the study conducted on an experimental alluvial fan by [1].

For the case study, the results obtained from the weighting procedure indicate that the criterion exerting the greatest influence on the Vulnerability of the exposed elements is the Process Impact. Consequently, the values of the vulnerability index will be primarily determined by this factor. It has to be reminded, that in other architectural contexts (i.e., buildings either featuring local protection measures or specifically designed for resistance) experts might have proposed both another Vulnerability model structure and a different set of weights for the considered influencing variables.

The obtained results indicate that buildings experiencing higher degrees of loss are situated in areas with high values of Specific Normal Force and at a short distance from the river's margins, typically within approximately 150 m, except for two houses located at distances of 364 and 511 m, respectively. Regarding the Building Materials, it is notable that buildings exhibiting very high and high vulnerability are primarily constructed with fibrocement and founded on concrete pillars. Regarding the type of foundation, it was also observed that despite experts considering slab foundations as a less influential structural feature during criteria weighting, they still exhibit high vulnerability values, likely due to their higher impact values (see Figure 12).

In addition to the damage mechanisms discussed by experts, [31] also highlight the potential impact of collisions with large wood logs and other floating objects, including tanks and vehicles. However, the effects stemming from this phenomenon have not been accounted for in the proposed model. Consequently, we strongly advocate for thorough consideration of this aspect in future studies.

While the proposed model explicitly considers the impacts of Morphological Change, upon closer examination, it becomes apparent that, in absolute terms, the simulation suggests that neither erosion nor deposition are particularly significant in terms of their magnitudes. However, given the substantial morphological alterations, such as channel avulsion and the incision of a new channel, observed during the 2008 event, the importance of this variable warrants careful evaluation.

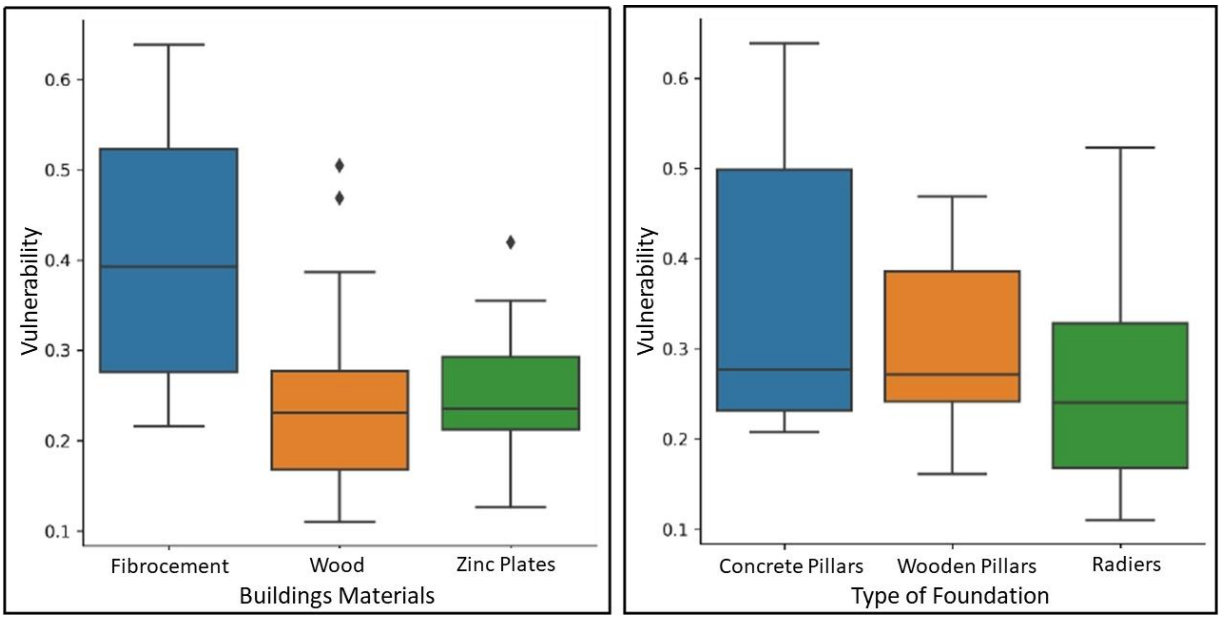

(A) (B)

Figure 12. Boxplots showing Vulnerability values by categories reflecting different building characteristics. (**A**) Differential effect on vulnerability exerted by the different Building Materials; (**B**) Differential effect on vulnerability exerted by the different Types of Foundation.

5. Conclusions

- We provide a method for Vulnerability assessment and subsequent Specific Risk analyses, which could be applied in areas affected by volcanic disturbances and in urban contexts with architectural typologies like those present in Chaitén in the south of Chile. Flood modeling and the physical characterization of building allowed us to get a detailed risk analysis of Chaitén identifying dozens of buildings of residential and no-residential use endangered by flows with non-negligible specific normal forces (i.e., > 400 N/m^2) and exposed to processes such as erosion and deposition.
- Our method requires high spatial resolution DEMs and imagery to be applied effectively as more detailed flow simulations can be achieved. Future methodological improvements may address the automatization of certain processes, such as delineating the potentially exposed residential buildings. In this case, new publicly available databases such as Open Buildings from Google can be used reducing time delineating buildings. Other task can be also automatized such as the extraction of maximum values of the considered Process Impact variables, quantifying the hydrodynamic Impact by also considering the effect of flow velocity, and optimizing the assessment of the Structural Characteristics and the employed Building Materials.
- In parallel, as experts indicated repeatedly, progress can be made on the one hand in developing physical process structure interaction models and on the other hand in corroborating the applicability of statistically based indicator-based approaches to provide a flexible set of tools for practitioners confronted with complex flood risks to be mitigated. Finally, our method proved to be useful in specific risk analysis related to floods in volcanic settings and can be adapted to assess risks in other geographical regions.

Author Contributions

Conceptualization: C.B.; B.M.; methodology: C.B.; B.M.; software: C.B.; P.I.; G.D.; D.B.; formal analysis: C.B.; D.B.; G.D.; investigation: C.B.; B.M.; writing - draft preparation: B.M.; writing -review and editing: B.M.; C.B.; P.I.; supervision: B.M.; funding acquisition - project administration: B.M.

Funding

ANID/FONDECYT Project Grant Nr. 1200091.

Institutional Review Board Statement

Not applicable.

Informed Consent Statement

Not applicable.

Data Availability Statement

Data will be made available upon kind request.

Acknowledgments

The research was funded by the ANID FONDECYT Project Nr. 1200091 "Unravelling the dynamics and impacts of sediment-laden flows in urban areas in southern Chile as a basis for innovative adaptation (SEDIMPACT)", led by Bruno Mazzorana.

The authors also acknowledge the help of Marcello Guittari for creating the video tutorials for the application of the AHP method and writing a report on the vulnerability of buildings within the SEDIMPACT Project. Pablo Iribarren also acknowledges project Anillo ACT210046 "Compound and cascading climate extremes in Chile".

Conflicts of Interest

The authors declare no conflict of interest.

References

1. Sturm, M.; Gems, B.; Keller, F.; Mazzorana, B.; Fuchs, S.; Papathoma Köhle, M; Aufleger, M. Experimental Analyses of Impact Forces on Buildings Exposed to Fluvial Hazards. *J. Hydrology* **2018**, *565,* 1–13.
2. Korswagen, P.; Longo, M.; Rots, J. Fragility Curves for Light Damage of Clay Masonry Walls Subjected to Seismic Vibrations. *Bull. Earthq. Eng.* **2022**, *20*, 1–35.
3. Mazzoleni, M.; Mård, J.; Rusca, M.; Odongo, V.; Lindersson, S.; Di Baldassarre, G. Floodplains in the Anthropocene: A Global Analysis of the Interplay Between Human Population, Built Environment, and Flood Severity. *W. Resources Res.* **2021**, *57*, e2020WR027744. [CrossRef]
4. Lavigne, F.; Jean-Claude, T. Sediment Transportation and Deposition by Rain-Triggered Lahars at Merapi Volcano, Central Java, Indonesia. *Geomorphology* **2003**, *49*, 45–69. [CrossRef]
5. Zingaretti, V.; Iroumé, A.; Llena, M.; Mazzorana, B.; Vericat, D.; Batalla, R.J. Geomorphological Evolution of the Blanco Este River after Recent Eruptions of the Calbuco Volcano. *Geomorphology* **2023**, *425*, 108570. [CrossRef]
6. Lavigne, F. Lahar Hazard Micro-Zonation and Risk Assessment in Yogyakarta city, Indonesia. *GeoJournal* **1999**, *49*, 173–183. [CrossRef]
7. Thouret, J.C.; Taillandier, M.; Arapa, E.; Wavelet, E. Vulnerable Settlements to Debris Flows in Arequipa, Peru: Population Characteristics, Hazard Knowledge, Risk Perception, and Disaster Risk Management. *Nat. Hazards* **2024**, 120, 901–955.
8. Una revisión de inundaciones fluviales en Chile período 1574 – 2012: causas, recurrencia y efectos geográficos. Available online: https://www.scielo.cl/scielo.php?pid=S0718-34022014000100012&script=sci_arttext (accessed on 01 October 2023).
9. Desastres por inundaciones fluviales en un área de expansión urbana: curso inferior de la cuenca del río Andalién-Chile central (1943 – 2011). Available online: https://www.researchgate.net/profile/Octavio-Rojas/publication/303804450_Desastres_por_inundaciones_fluviales_en_un_area_de_expansion_urbana_curso_inferior_de_la_cuenca_del_rio_Andalien_Chile-Central_1943-2011/links/57536a4c08ae17e65ec6cc99/Desastres-por-i (accessed on 15 April 2023).
10. Viale, M.; Valenzuela, R.; Garreaud, R.D.; Ralph, F.M. Impacts of Atmospheric Rivers on Precipitation in Southern South America. *J. Hydrometeorology* **2018**, *19*, 1671–1687.

11. Pallister, J.; Diefenbach, A.; Burton, W.; Muñoz, J.; Griswold, J.; Lara, L.; Lowenstern, J.; Valenzuela, C. The Chaitén rhyolite lava dome: Eruption Sequence, Lava dome volumes, Rapid Effusion Rates and Source of the Rhyolite Magma. *Andean Geol.* **2013**, *40*, 277–294.
12. Ulloa, H.; Iroumé, A.; Picco, L.; Korup, O.; Aristide, M.; Mao, L.; Ravazzolo, D. Massive Biomass Flushing Despite Modest Channel Response in the Rayas River Following the 2008 Eruption of Chaitén volcano, Chile. *Geomorphology* **2015**, *250*, 397–406.
13. Mazzorana, B.; Picco, L.; Rainato, R.; Iroumé, A.; Ruiz-Villanueva, V.; Rojas, C.; Valdevenito, G.; Iribarren-Anacona, P.; Melnick, D. Cascading Processes in a Changing Environment: Disturbances on Aluvial Ecosystems in Chile and Implications for Hazard and Risk Management. *Sci. Total Environ.* **2019**, *655*, 1089–1103.
14. Mazzorana, B.; Levaggi, L.; Keiler, M.; Fuchs, S. Towards Dynamics in Flood Risk Assessment. *Nat. Hazards Earth Syst. Sci.* **2012**, *12*, 3571–3587.
15. *Manual para la elaboración de mapas de riesgo.* Available online: https://www.mininterior.gov.ar/planificacion/pdf/Manual-elaboracion-mapas-riesgo.pdf (accessed on 20 November 2022). [CrossRef]
16. Jonkman, S.N.; van Gelder, P.H.A.J.M.; Vrijling, J. A Overview of Quantitative Risk Measures for Loss of Life and Economic Damage. *J. Hazard. Mater.* **2003**, *99*, 1–30. [CrossRef]
17. Riesgos naturales: evolución y modelos conceptuales. Available online: http://www.scielo.org.ar/scielo.php?pid=S1852-42652011000100005&script=sci_arttext (accessed on 17 August 2023).
18. Fuchs, S. Susceptibility Versus Resilience to Mountain Hazards in Austria—Paradigms of Vulnerability Revisited. *Nat. Hazards Earth Syst. Sci.* **2009**, *9*, 337–352.
19. Mazzorana, B.; Fuchs, S. Fuzzy Formative Scenario Analysis for Woody Material Transport Related Risks in Mountain Torrents. E*nvironmental Modelling Softw.* **2010**, *25*, 1208–1224.
20. Estudio del Impacto Territorial-Ambiental Generado por la Erupción del Volcán Chaitén. Tesis de Pregrado. Available online: https://repositorio.uchile.cl/handle/2250/100349 (accessed on 20 December 2023).
21. Estimación holística del riesgo sísmico utilizando sistemas dinámicos complejos. Available online: https://upcommons.upc.edu/handle/2117/93531 (accessed on 7 July 2024).
22. Mazzorana, B.; Simoni, S.; Scherer, B.; Gems, B.; Fuchs, S.; Keiler, M. A Physical Approach on Flood Risk Vulnerability of Buildings. *Hydrol. Earth Syst. Sci.* **2014**, *18*, 3817–3836.
23. Lara, L. The 2008 Eruption of the Chaitén Volcano, Chile: A Preliminary Report. *Andean Geol*. **2009**, *36*, 125–130.
24. Major, J.; Lara, L. Overview of Chaitén Volcano, Chile, and Its 2008–2009 Eruption. *Andean Geol.* **2013**, *40*, 196–215.
25. Major, J. J.; Bertin, B.; Pierson, T.C.; Amigo, A.; Iroumé, A.; Ulloa, H.; Castro, J. Extraordinary sediment delivery and rapid geomorphic response following the 2008–2009 eruption of Chaitén Volcano, Chile. *Water. Resour. Res.* **2016**, 52, 5075–5094. [CrossRef]
26. Pierson, T.C.; Major, J.J.; Amigo, A.; Moreno, H. Acute Sedimentation Response to Rainfall Following the Explosive Phase of the 2008–2009 Eruption of Chaitén volcano, Chile. *Bull. Volcanology* **2013**, *75*, 1–17.
27. Swanson, F.J.; Jones, J.A.; Crisafulli, C.; Lara, A., 2013. Effects of Volcanic and Hydrologic Processes on Forest Vegetation, Chaitén Volcano, Chile. *Andean Geol*. **2013**, *40*, 359–391.
28. Ruiz-Villanueva, V.; Mazzorana, B.; Bahamondes, D., Rojas, I. Cascading Processes and Multiple Hazards and Risks in Chilean Rivers: Lessons Learnt and Remaining Challenges. In *Rivers of Southern and Patagonia*; Oyarzún, C., Mazzorana, B., Iribarren-Anacona, P., Iroumé, A. Eds.; Springer Cham: Gewerbestrasse, Switzerland, 2023; pp. 235–250.
29. Basso-Báez, S.; Mazzorana, B.; Ulloa, H.; Bahamondes, D.; Ruiz-Villanueva, V.; Sanhueza, D.; Iroumé, A.; Picco, L. Unravelling the Impacts to the Built Environment Caused by Floods in a River Heavily Perturbed by Volcanic Eruptions. *J. South Am. Earth Sci.* **2020**, *102*, 102655.
30. Gefährdungs-und Schadensbilder für Gebäude. Available online: https://link.springer.com/chapter/10.1007/978-3-7091-0681-5_3 (accessed on 24 March 2023).
31. Papathoma-Köhle, M.; Gems, B.; Sturm, M.; Fuchs, S. Matrices, Curves and Indicators: A Review of Approaches to Assess Physical Vulnerability to Debris Flows. *Earth-Sci. Rev.* **2017**, *171*, 272–288.
32. Centro de Información de Recursos Naturales. Avaible Online: https://www.sitrural.cl/wp-content/uploads/2020/03/Chaiten_rec_nat_proy.pdf (accessed on 7 December 2017).
33. Martini, L.; Picco, L.; Iroumé, A.; Cavalli, M. Sediment Connectivity Changes in an Andean Catchment Affected by Volcanic Eruption. *Sci. Total Environ.* **2019**, *692*, 1209–1222. [CrossRef]
34. Estrategia para la inferencia causal y planificación de estudios observacionales en las ciencias sociales: el caso de Chaitén post erupción del 2008. Available online: https://www.scielo.cl/scielo.php?pid=S0718-090X2016000300010&script=sci_arttext (accessed on 17 July 2023).

35. Atanasova-Pachemska, T.; Lapevski M.; Timovski, R. Analytical Hierarchical Process (AHP) Method Application in the Process of Selection and Evaluation. In Proceedings of the International Scientific Conference, Gabrovo, Bulgaria, 22 November 2014.
36. Ibrahim, A.; Tiki, D.; Mamdem, L.; Leumbre, O.; Bitom, D.; Lazar, G. MultiCriteria Analysis (MCA) Approach and GIS for Flood Risk Assessment and Mapping in Mayo Kani Division, Far North Region of Cameroon. *International J. Advanced Remote. Sensn. GIS.* **2018**, *7*, 2793–2808.
37. Goepel, K. Implementing the Analytic Hierarchy Process as a Standard Method for Multi-Criteria Decision Making in Corporate Enterprises—A New AHP Excel Template with Multiple Inputs. In Proceedings the International Symposium on the Analytic Hierarchy Process, Kuala Lumpur, Malaysia, 23–36 June 2013.
38. Explorando la respuesta hidrodinámica de un río altamente perturbado por erupciones volcánicas: el Río Blanco, Chaitén (Chile). Available online: https://iwaponline.com/IA/article/27/2/73/95547 (accessed on 15 August 2023).
39. Graham, D.; Rice, S.; Reid, I. A Transferable Method for the Automated Grain Sizing of River Gravels. *Water Resour. Res.* **2005**, *41*. [CrossRef]
40. Detert, M.; Weitbrecht, V. User Guide to Gravelometric Image Analysis by BASEGRAIN. *Adv. Sci. Res.* **2013**, 1789–1795.
41. Chow, V. *Open-Channel Hydraulics*. McGraw-Hill: New York, USA, 1959; pp. 89–148.
42. Iber: herramienta de simulación numérica del flujo en ríos. Available online: https://www.sciencedirect.com/science/article/pii/S0213131512000454 (accessed on 12 January 2024).
43. Análisis de riesgo específico de inundación de la ciudad de Chaitén, bajo un escenario de crecida extrema del río Blanco, post erupción. Available online: https://www.scielo.cl/scielo.php?script=sci_arttext&pid=S0718-22442015000300003 (accessed on 15 March 2024).
44. Mazzorana, B.; Maturana, F. Mitigating Complex Flood Risks in Southern Chile in a Particular Spatial Planning Context: Towards a Sustainable Strategy. In *Rivers of Southern and Patagonia*; Oyarzún, C., Mazzorana, B., Iribarren-Anacona, P., Iroumé, A. eds; Springer Cham: Gewerbestrasse, Switzerland, 2023; pp. 193–233.
45. Papathoma-Köhle, M.; Schlögl, M.; Fuchs, S. Vulnerability Indicators for Natural Hazards: An Innovative Selection and Weighting Approach. *Sci. Rep.* **2019**, *9*, 15026.